

Entrance channel effects by populating resonances in the ^{26}Al , ^{29}Si , and ^{30}Si systems

R. L. Parks and S. T. Thornton

*Department of Physics, University of Virginia, Charlottesville, Virginia 22901
and Max-Planck-Institut für Kernphysik, 6900 Heidelberg, Federal Republic of Germany*

K. R. Cordell and C.-A. Wiedner

*Max-Planck-Institut für Kernphysik, 6900 Heidelberg, Federal
Republic of Germany*

(Received 16 July 1981)

Excitation functions have been measured for the elastic, recoil, and alpha-particle exit channels for four reactions: $^{17}\text{O} + ^{12}\text{C}$ ($E_{\text{lab}} = 30.0 - 57.0$ MeV), $^{16}\text{O} + ^{13}\text{C}$ ($E_{\text{lab}} = 29.5 - 52.6$ MeV), $^{17}\text{O} + ^{13}\text{C}$ ($E_{\text{lab}} = 30.0 - 57.0$ MeV), and $^{16}\text{O} + ^{10}\text{B}$ ($E_{\text{lab}} = 42.4 - 60.1$ MeV). The alpha particles were detected at $\theta_{\text{lab}} = 10^\circ$ while the elastic and recoil particles were detected at $\theta_{\text{lab}} = 34^\circ$. Statistical analyses of the data are used to search for correlated, nonstatistical structures in the excitation functions. The resonant properties of three compound nuclei (^{26}Al , $^{29,30}\text{Si}$) are studied by comparing the excitation energies at which nonstatistical structures are seen when the nuclei are formed via different well matched (in terms of J_{max}) entrance channels. These resonancelike structures seen in the various entrance channels (for a given compound nucleus) are found to be uncorrelated in excitation energy, thereby implying a dependence upon the properties of the entrance channel. The lack of entrance channel correlations and the short lifetimes of the structures seen are viewed as evidence that the reaction may proceed through a quasimolecule, or that the compound nucleus itself is so highly excited and deformed that its formation is entrance channel dependent.

NUCLEAR REACTIONS $^{12}\text{C}(^{17}\text{O}, ^{17}\text{O})$, $(^{17}\text{O}, ^{12}\text{C})$, $(^{17}\text{O}, \alpha)$, $E = 30.0 - 57.0$ MeV; $^{13}\text{C}(^{16}\text{O}, ^{16}\text{O})$, $(^{16}\text{O}, ^{13}\text{C})$, $(^{16}\text{O}, \alpha)$, $E = 29.5 - 52.6$ MeV; $^{13}\text{C}(^{17}\text{O}, ^{17}\text{O})$, $(^{17}\text{O}, ^{13}\text{C})$, $(^{17}\text{O}, \alpha)$, $E = 30.0 - 57.0$ MeV; $^{10}\text{B}(^{16}\text{O}, ^{16}\text{O})$, $(^{16}\text{O}, ^{10}\text{B})$, $(^{16}\text{O}, \alpha)$, $E = 42.4 - 60.1$ MeV. Measured $\sigma(E)$ at $\theta_{\text{lab}} = 10^\circ$ for α and $\sigma(E)$ at $\theta_{\text{lab}} = 34^\circ$ for elastic and recoil. Natural ^{12}C target; enriched ^{13}C and ^{10}B targets. Resolution ~ 100 keV for α , 400–600 keV for elastic and recoil. Statistical and Hauser-Feshbach analyses. Entrance channel comparisons. Discussion of reaction mechanism.

I. INTRODUCTION

One of the most interesting and fundamental challenges to arise from the study of heavy-ion collisions at bombarding energies well above the Coulomb barrier is that of understanding and describing the nature and properties of the compound nucleus. Indeed, the validity of the classical conception of an equilibrated, long-lived nucleus in which all nucleons share the available energy and angular momentum must be questioned in the regime of high excitation energies (E^*) available to experimentalists today. The occurrence of reso-

nances in many light heavy-ion systems has served to focus a great deal of attention on this question since it is not altogether clear whether resonances are a signature of compound nucleus formation or depend mostly upon the entrance and/or exit channels. The work presented in this paper addresses the compound nucleus versus entrance channel effect aspect of heavy-ion reactions by searching for resonances correlated in different entrance channels leading to the same compound nucleus.

The first evidence for nonstatistical (resonance) structure was found in the $^{12}\text{C} + ^{12}\text{C}$ system^{1,2} and was strongly correlated in many exit channels and

at many angles. Thereafter, other systems comprised of α -conjugate nuclei, particularly the $^{16}\text{O} + ^{16}\text{O}$ and $^{16}\text{O} + ^{12}\text{C}$ systems,³ showed resonance structure. This prompted a search for resonances in systems in which at least one reactant was not α -like. For example, the $^{13}\text{C} + ^{12}\text{C}$ system received a great deal of attention⁴⁻⁷ but, although displaced only one neutron from the strongly resonating $^{12}\text{C} + ^{12}\text{C}$ system, initially showed little or no evidence for nonstatistical structure. The $^{14}\text{N} + ^{14}\text{N}$ system was also studied, partially to see if resonances were related to the collision of identical particles and also as a comparison for the $^{16}\text{O} + ^{12}\text{C}$ system.⁸ Excitation functions from the $^{14}\text{N}(^{14}\text{N},\alpha)^{24}\text{Mg}$ reaction were essentially structureless. In fact, many high spin states populated in ^{24}Mg by the $^{16}\text{O}(^{12}\text{C},\alpha)^{24}\text{Mg}$ reaction were not even seen in the $^{14}\text{N} + ^{14}\text{N}$ data. Some of the published work which showed resonances in non- α -conjugate systems was somewhat controversial and not verified in subsequent experiments. As a result, some reviews of the subject^{9,10} concluded that there were no proven resonances in any non- α -conjugate nuclei.

Aiding in the controversy at the time was the lack of a rigorous definition of a resonance. A large number of papers presented so-called evidence for resonances which was essentially nothing more than a visual correlation. Nearly every bump in a summed excitation function was said to represent a nonstatistical process. Unfortunately, very few calculations were done to see if, in fact, the behavior observed was actually inconsistent with statistical model predictions. As a result, many alleged findings of resonance structure were distrusted and especially so for the non- α -conjugate systems because what little structure had been seen was much weaker than that of the α -conjugate systems.

Even so, measurements involving non- α -conjugate nuclei continued and, at the same time, the problem of discerning ordinary statistical fluctuations from true resonance structure was addressed. In order to make precise judgments of structures seen in excitation functions, we adopted a set of fairly rigorous criteria. A description of such criteria and their application to experimental data are seen, for example, in the paper by Dennis *et al.*¹¹ We have also searched for resonances in non- α -conjugate systems such as $^{14}\text{N} + ^{12}\text{C}$ (Refs. 11 and 12), $^{13}\text{C} + ^{12}\text{C}$ (Ref. 7), and $^{12}\text{C} + ^9\text{Be}$ (Ref. 13).

A number of other non- α -conjugate systems were studied and analyzed by other groups also us-

ing more rigorous criteria. Surprisingly, many of these searches revealed structures which were found to be nonstatistical. It is now clear that resonances have been seen by several different experimental groups in several non- α -conjugate systems at energies above the Coulomb barrier, e.g., $^{18}\text{O} + ^{12}\text{C}$, $^{16}\text{O} + ^{14}\text{C}$, $^{14}\text{N} + ^{12}\text{C}$, $^{12}\text{C} + ^9\text{Be}$, $^{12}\text{C} + ^{11}\text{B}$, and $^{15}\text{N} + ^{12}\text{C}$ (see Refs. 7 and 11-18).

One of the remaining questions of interest is why resonances exist in some systems and not in others. Most of the early models proposed mechanisms which might be responsible for resonances, but had little or no provision for selecting which systems are most likely to resonate. A recent model by Thornton *et al.*¹⁹ suggests that the binding energies of the entrance channel nuclei and their effective moment of inertia are the dominant factors. A similar conclusion was drawn by Baye in a discussion of heavier systems ($A \sim 52$).²⁰ This implies a heavy dependence upon the properties of the incoming nuclei as opposed to those of the compound nucleus, thereby prompting the experimental investigation of whether the existence of a resonance is evidence for compound nucleus formation or merely a dynamical entrance channel effect.

The work presented in this paper was prompted by some of the very fundamental questions described above. In particular, we chose to address experimentally three questions pertaining to the resonance phenomenon:

(1) Can resonances exist at high excitation energies (two to three times the Coulomb barrier) in the compound nucleus? It is thought that at very high excitation energies, many more channels are available for decay and that any nonstatistical structure may be averaged out.

(2) Are there more non- α -conjugate systems which exhibit resonance behavior? Based on calculations in Ref. 19, there are such systems which are likely candidates due to the possibility of populating isolated states in a region of low level density. (See Sec. IV for more details.)

(3) How strongly is resonance behavior dependent upon the entrance channel? Correlations between exit channels have been well documented² for some reactions but correlations between entrance channels have not been widely observed. This is related to the question of whether or not resonances are a compound nucleus effect.

We have pursued these questions by measuring excitation functions for $^{17}\text{O} + ^{12}\text{C}$, $^{16}\text{O} + ^{13}\text{C}$,

$^{16}\text{O} + ^{10}\text{B}$, and $^{17}\text{O} + ^{13}\text{C}$ over a range of high excitation energies. While questions (1) and (2) are quite obviously addressed by these measurements, question (3) is probed by making measurements on: (a) the $^{17}\text{O} + ^{12}\text{C}$ and $^{16}\text{O} + ^{13}\text{C}$ systems over the same E^* (^{29}Si), (b) the $^{16}\text{O} + ^{10}\text{B}$ system over the same E^* (^{26}Al) covered in an earlier experiment on $^{14}\text{N} + ^{12}\text{C}$ (Ref. 12), and (c) the $^{17}\text{O} + ^{13}\text{C}$ system over the same E^* (^{30}Si) previously measured for the $^{18}\text{O} + ^{12}\text{C}$ and $^{16}\text{O} + ^{14}\text{C}$ entrance channels.^{17,18}

The experimental procedure and results are found in Sec. II. The use of several statistical tests on their application to the present data are discussed in Sec. III. A review of theoretical models and entrance channel comparisons are found in Sec. IV, with final conclusions and a summary in Sec. V.

II. EXPERIMENTAL PROCEDURE

The oxygen beams were obtained from the MP tandem Van de Graaff accelerator at the Max-Planck-Institut für Kernphysik, Heidelberg. The ^{17}O ions were accelerated to 30.0–57.0 MeV for the $^{17}\text{O} + ^{13}\text{C}$ and $^{17}\text{O} + ^{12}\text{C}$ reactions, whereas the ^{16}O ions were accelerated to 29.5–52.6 MeV for the $^{16}\text{O} + ^{13}\text{C}$ reaction and 42.4–60.1 MeV for the $^{16}\text{O} + ^{10}\text{B}$ reaction. Beam intensities varied from 0.2 to 1.5 μA (electrical) depending on count rate due to the given combination of cross section and target thickness. The current of the beam after traversing the target was measured with a Faraday cup incorporating an electron suppressor element. Typical charge collection for one run was 1–2 mC.

All targets were self-supporting foils whose thicknesses were chosen to optimize the usual count rate/resolution trade-off. The natural ^{12}C targets ranged in thickness from 27–33 $\mu\text{g}/\text{cm}^2$, which represents an energy loss of 150–200 keV (lab) with the ^{17}O beam. The ^{13}C targets (enriched to $\sim 95\%$) had thicknesses of 48–53 $\mu\text{g}/\text{cm}^2$, corresponding to an energy loss of 200–300 keV (lab) with the ^{17}O beams. The ^{10}B target (enriched to $\sim 95\%$) had a thickness of 78 $\mu\text{g}/\text{cm}^2$, causing an energy loss of 380–500 keV (lab). All target thicknesses were checked both before and after the experiments by measuring the energy loss of α particles from a thin ^{241}Am source. A small amount of carbon buildup ($\sim 5\%$) was detected during some of the early $^{17}\text{O} + ^{12}\text{C}$ measurements when the scattering chamber pressure ($\sim 5 \times 10^{-6}$ Torr)

was higher than normal. Even this small buildup was closely monitored so that the thickness of the ^{12}C target as a function of time could be determined and taken into account in the absolute cross section calculations. For the three reactions which did not require ^{12}C , this buildup was much reduced due to an improved vacuum of $\sim 1 \times 10^{-6}$ Torr. A new target spot was used when the ^{12}C buildup became significant.

Excitation functions for three exit channels were measured for each reaction: alpha, elastic, and recoil particles. Table I indicates the energies and angles at which measurements were made. Note that for each reaction, the first row lists reaction parameters in the laboratory system and the second row lists them in the center-of-mass system.

The elastic and recoil particles were detected using a ΔE - E telescope (ionization chamber, surface-barrier detector) with a solid angle of 0.40 msr positioned at $\sim 34^\circ$ (lab) in the scattering chamber. We were unable to cleanly resolve any inelastic states because: (i) target impurities caused interference and identification problems in the energy spectra and (ii) energy resolution due to target thickness and angular acceptance of the telescope was not sufficient. Finally, the inelastic states were not strongly excited at the energies under investigation. Even so, by detecting the elastic and recoil particles, one obtains the equivalent of two different angles in the center-of-mass system for elastic scattering (see Table I).

The α particles at 10° (lab) were momentum-analyzed by a quadrupole-three-dipole (Q3D) magnetic spectrograph with a solid angle of ~ 10 msr and were detected at the focal plane by a 1.4 m position sensitive proportional counter (PSPC). This particular detector-spectrograph configuration and its associated electronics are described in detail in the literature.²¹ We use the PSPC with a 25 μm thick aluminized Mylar entrance foil and a P -10 gas pressure of 580 Torr. The α particles could easily be identified by their energy loss in the ΔE section of the PSPC.

Excitation functions for approximately 12 groups of α particles were measured, corresponding to different final states in the residual nucleus. Typical α spectra are shown in Fig. 1 for the four reactions. Resolution of a single final state was 80–120 keV (c.m.), which is consistent with estimates based on straggling and energy loss in the target and the PSPC. The states in Fig. 1 appear to be broad but this is simply an artifact of the large dispersion of the Q3D. Such dispersion

TABLE I. Experimental parameters for the four reactions studied.

Reaction	Bomb. energy (MeV)	Ex. energy ^a (MeV)	Energy step (MeV)	$\theta(\alpha)^b$ (deg)	$\theta_1(\text{el})^c$ (deg)	$\theta_2(\text{el})^d$ (deg)
$^{17}\text{O} + ^{12}\text{C}$	30.0–57.0 (lab)		0.50	10.0	35	41
	12.4–23.6 (c.m.)	33.5–44.7	0.21	14.0	89	110
$^{16}\text{O} + ^{13}\text{C}$	29.5–52.6 (lab)		0.30	10.0	33	48
	13.2–23.6 (c.m.)	33.5–43.9	0.13	13.9	75	114
$^{17}\text{O} + ^{13}\text{C}$	30.0–57.0 (lab)		0.50	10.0	35	44
	13.0–24.7 (c.m.)	39.8–51.5	0.22	13.4	84	110
$^{16}\text{O} + ^{10}\text{B}$	42.4–60.1 (lab)		0.30	10.0	33	38
	16.3–23.1 (c.m.)	35.8–42.6	0.12	14.6	94	114

^aExcitation energies refer to the compound nucleus for each of the four reactions i.e., ^{29}Si , ^{29}Si , ^{30}Si , ^{26}Al .

^b $\theta(\alpha)$ is the angle at which the α particles were detected.

^c $\theta_1(\text{el})$ is the angle at which elastic particles were detected directly.

^d $\theta_2(\text{el})$ is the angle for elastic particles which corresponds to detecting the recoil particles at angle $\theta_1(\text{el})$.

makes the separation of multiplets easier, but at the same time greatly limits the number of states which fall kinematically within the dynamic range of the spectrograph.

All data were acquired with an on-line Nuclear Data 6660 computer. The α -particle spectra were stored in 1024 channel arrays while the ΔE - E signals for the elastic and recoil data were binned into 64×256 channel arrays. Both the one- and two-dimensional spectra could be displayed live during the experiment in order to make the usual checks on the incoming data. These data were later analyzed off-line using a PDP 11/34 computer.

Figures 2–5 show the excitation functions measured for the four reactions under consideration. The absolute cross sections have uncertainties of about 20% while the relative uncertainties are about 5%. Note that a few of the excitation functions are incomplete at the low energy end because the α particles corresponding to these states could not reach the detector kinematically.

Figure 2 shows 12 excitation functions for the $^{17}\text{O} + ^{12}\text{C}$ reaction. Ten of these correspond to states in the ^{25}Mg residual nucleus for the α -particle exit channel while the other two are elastic scattering measurements at c.m. angles of 89° and 110°. The ten ^{25}Mg groups actually represent 16 states because several multiplets could not be resolved.

Figure 3 shows ten excitation functions for the $^{16}\text{O} + ^{13}\text{C}$ reaction. Eight of these correspond to 14 states in the ^{25}Mg residual nucleus for the α -particle exit channel while the other two are elastic scattering at c.m. angles of 75° and 114°.

Figure 4 shows ten excitation functions for the $^{17}\text{O} + ^{13}\text{C}$ reaction. Eight of these correspond to 12 states in the ^{26}Mg residual nucleus for the α -particle exit channel while the other two are elastic scattering at c.m. angles of 84° and 110°.

Figure 5 shows ten excitation functions for the $^{16}\text{O} + ^{10}\text{B}$ reaction. Nine of these correspond to 11 states in the ^{22}Na residual nucleus for the α -particle exit channel. The last excitation function is an elastic scattering measurement at $\theta_{\text{c.m.}} = 94^\circ$. The recoil ^{10}B particles were also detected (equivalent to elastic particles at $\theta_{\text{c.m.}} = 114^\circ$) but these were very low in energy. The resulting energy spectra were rather flat with no resolvable recoil peak, so there is no excitation function corresponding to this measurement.

III. STATISTICAL ANALYSIS AND RESULTS

All the excitation functions except the elastics exhibit characteristic fluctuations. Absolute, energy-averaged cross sections have been calculated for the α -particle exit channel using the Hauser-Feshbach computer code HELGA as described in Refs. 22 and 23. The calculated cross sections agree reasonably well with all of the data. An example of these results is seen in Fig. 5, where the dashed lines are the HELGA calculations. This agreement with HELGA implies that compound nuclear formation dominates the transitions observed.

The absolute normalization was generally reproduced well with HELGA by inputting I_{max} as calcu-

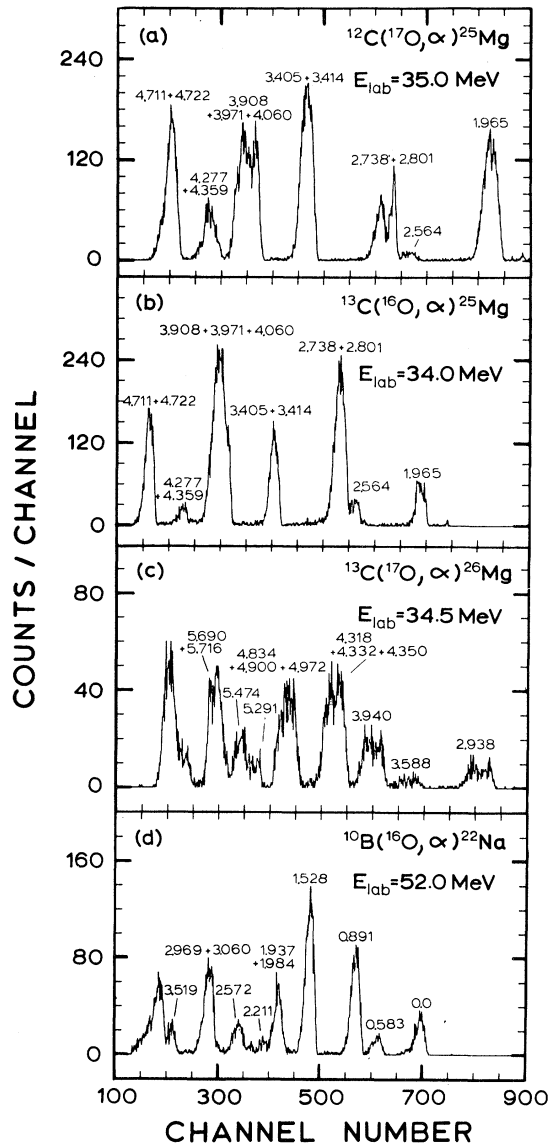


FIG. 1. Typical energy spectra from the Q3D for the α -particle exit channel for the following reactions: (a) $^{17}\text{O} + ^{12}\text{C}$, (b) $^{16}\text{O} + ^{13}\text{C}$, (c) $^{17}\text{O} + ^{13}\text{C}$, and (d) $^{16}\text{O} + ^{10}\text{B}$. All spectra were measured at $\theta_{\text{lab}} = 10^\circ$. States in the residual nucleus are identified.

lated from the formalism of Wilczynski.²⁴ The level density and pairing energy parameters were taken from Gilbert and Cameron²⁵ whenever possible. The optical model potentials for the n , p , d , ^3He , and ^4He exit channels are found in Perey and Perey²⁶ while the potentials for the heavy-ion exit

channels were taken from Greenwood *et al.*²⁷

The detection of nonstatistical structure in a set of fluctuating cross sections can be a difficult problem. In a system such as $^{12}\text{C} + ^{12}\text{C}$, the resonance structures are quite strong and easily correlated, even by eye. However, the structures seen in non- α -conjugate systems tend to be considerably weaker. Even so, if a visually weak structure is correlated in many reaction channels, then it may in fact be highly nonstatistical. The key realization is that any suspected structure *must* be compared to the statistical model if we intend to judge whether or not it is nonstatistical.

A. Statistical tests

A number of tests exist which are used to detect nonstatistical structure. Our experience has been that no single test is absolutely reliable under all conditions. Instead we use the results of four tests in order to critically assess the properties of a given structure. These tests are the deviation function, the energy-dependent cross-correlation function, the distribution of maxima test, and the sum of the excitation functions. Each test has its own strengths and weaknesses, as discussed in Ref. 11. We shall briefly review here the use and interpretation of these tests.

The deviation function is simply a sum of differences of the excitation functions from a running average. For N excitation functions the formulation is

$$D(E) = \frac{1}{N} \sum_{i=1}^N \left[\frac{\sigma_i(E)}{\langle \sigma_i(E) \rangle} - 1 \right], \quad (1)$$

where $\langle \sigma_i(E) \rangle$ is a running average for excitation function i . It is obvious that a maximum or minimum which occurs near the same energy in several of the excitation functions will be quite evident in $D(E)$. Unfortunately, if even one excitation function should have a very strong maximum or minimum, this too will show up in $D(E)$. The main shortcoming of $D(E)$ is that a weak but highly correlated structure may produce a deviation which is less prominent than what would be caused by an ordinary fluctuation in one excitation function.

The energy-dependent cross-correlation function for N excitation functions is defined as

$$C(E) = \frac{2}{N(N-1)} \sum_{i>j=1}^N \left[\frac{\sigma_i(E)}{\langle \sigma_i(E) \rangle} - 1 \right] \left[\frac{\sigma_j(E)}{\langle \sigma_j(E) \rangle} - 1 \right] [R_i(0)R_j(0)]^{1/2}, \quad (2)$$

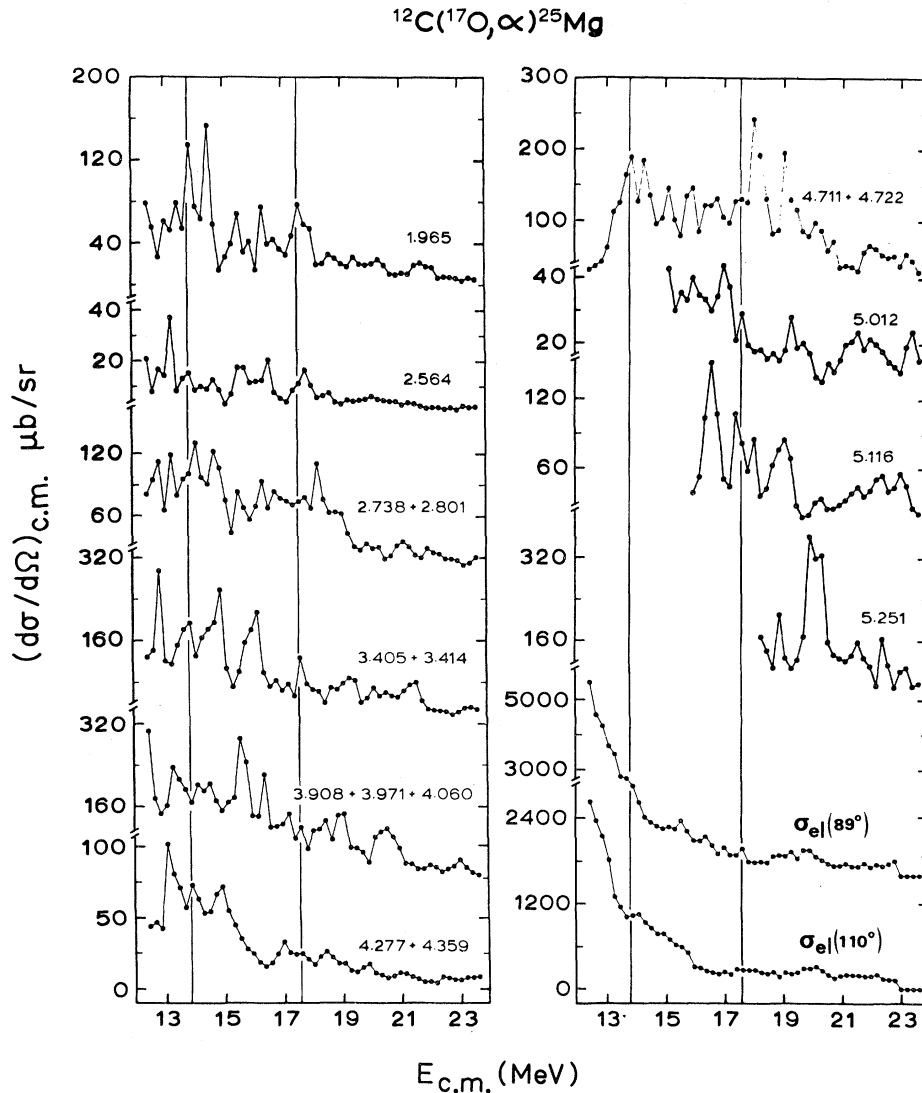


FIG. 2. Excitation functions for the $^{17}\text{O} + ^{12}\text{C}$ reaction for the elastic ($\theta_{\text{c.m.}}=89^\circ, 100^\circ$) and α -particle ($\theta_{\text{c.m.}}=14.0^\circ$) exit channels. The excitation energies of the residual states in ^{25}Mg are indicated. The solid lines (see Sec. III) show the location of nonstatistical structure.

where $R_i(0) = \langle \langle \sigma_i^2(E) / \langle \sigma_i(E) \rangle^2 - 1 \rangle \rangle_{\text{av}}$ and $\langle \langle \rangle \rangle_{\text{av}}$ indicates an average over the excitation function i . This function is very instructive because its magnitude at each energy is determined by the *correlation* of maxima and minima in the excitation functions, not by differences as in $D(E)$. Unfortunately, $C(E)$ is not strictly bounded by ± 1 and thus cannot be compared directly to the predictions of the statistical model. Additionally, care must be exercised because $C(E)$ is somewhat sensitive to the averaging interval E_{int} , used in the running average $\langle \sigma_i(E) \rangle$. For $E_{\text{int}} < 2$ MeV (c.m.), we

find that $C(E)$ depends strongly on E_{int} , but for $2.5 < E_{\text{int}} < 3.5$ MeV (c.m.), the dependence of $C(E)$ on E_{int} is nearly removed. Even given its limitations, $C(E)$ has been a valuable tool in our work because a truly nonstatistical structure normally produces a large correlation in comparison to the surrounding, supposedly uncorrelated, Ericson fluctuations.

The distribution of maxima test is based on counting the number of maxima which occur near the same excitation energy in a group of excitation functions. Clearly, if a resonance is present, it will

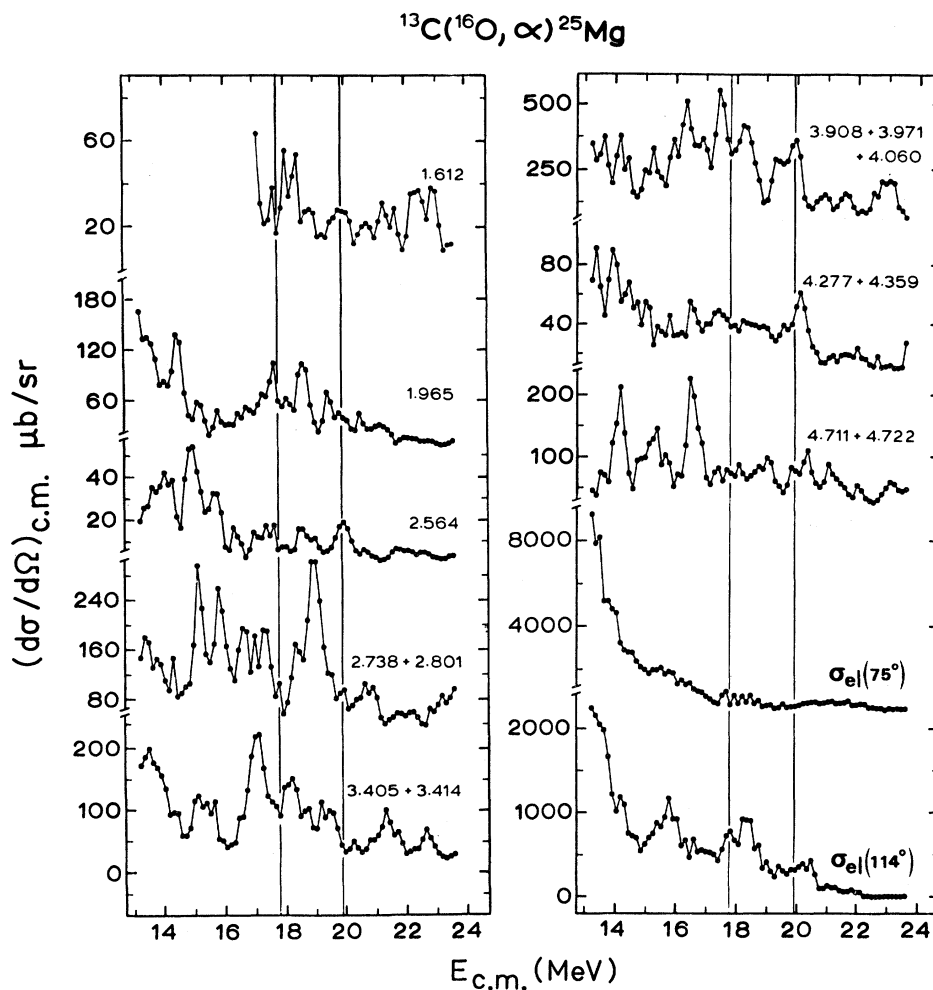


FIG. 3. Excitation functions for the $^{16}\text{O} + ^{13}\text{C}$ reaction for the elastic ($\theta_{\text{c.m.}} = 75^\circ, 114^\circ$) and α -particle ($\theta_{\text{c.m.}} = 13.9^\circ$) exit channels. The excitation energies of the residual states in ^{25}Mg are indicated. The solid lines (see Sec. III) show the location of nonstatistical structure.

manifest itself by producing an anomalously high number of maxima at a given excitation energy region in a group of excitation functions. A maximum is defined here as a point for which $\sigma_i(E) / \langle \sigma_i(E) \rangle$ is greater than some reference value r , and which is also significantly higher than its nearest neighbors. Usually the distribution of maxima test is conducted for a range of r values from 0.5 to 1.5. Note that a minimum can also be detected by negating the excitation functions and then performing the distribution of maxima test again.

The distribution of maxima test is also of great value because it may be used to judge whether or not a structure is inconsistent with the statistical model. This is done by calculating the probability

of observing N or more maxima in N_m excitation functions using

$$P(N) = \sum_{k=N}^{N_m} \frac{N_m! p^k (1-p)^{N_m-k}}{k!(N_m-k)!}, \quad (3)$$

where p is the probability parameter for the binomial distribution and can be determined from the data by counting the number of maxima in all excitation functions and dividing by the total number of points. We have adopted the convention of calling an event with a distribution of maxima probability of less than n^{-1} (where n is the number of points in each excitation function, typically $n^{-1} \sim 0.01$) nonstatistical based on the simple sta-

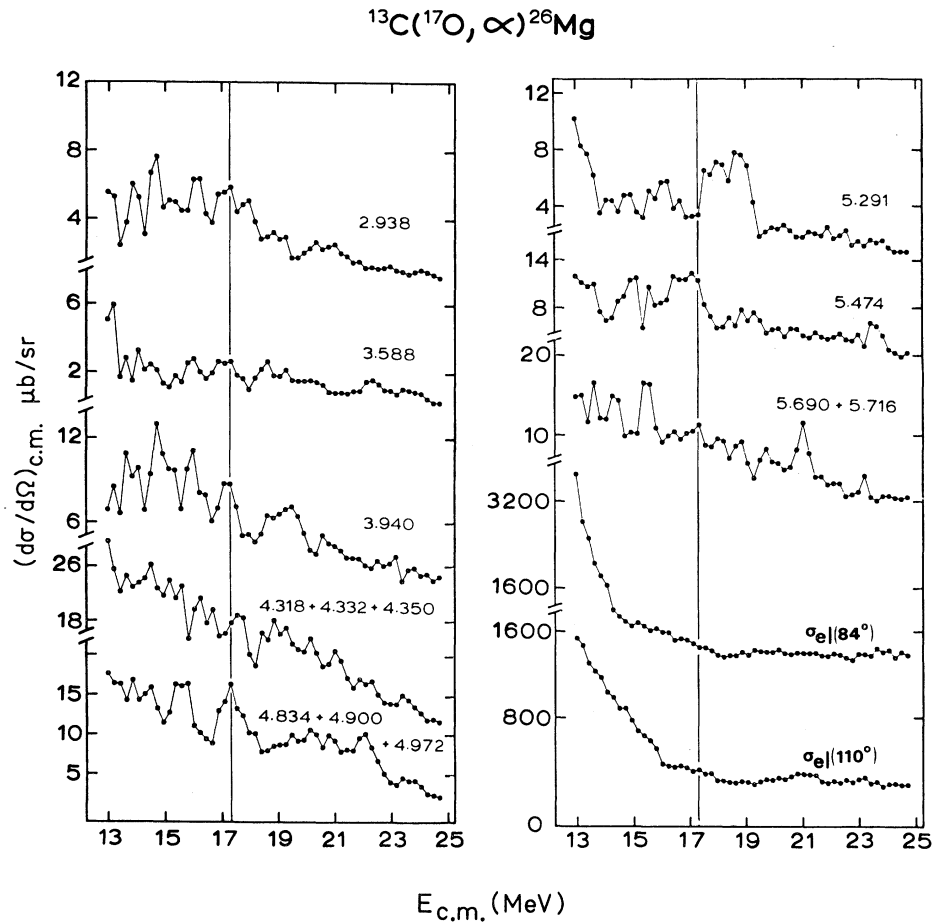


FIG. 4. Excitation functions for the $^{17}\text{O} + ^{13}\text{C}$ reaction for the elastic ($\theta_{\text{c.m.}} = 84^\circ, 110^\circ$) and α -particle ($\theta_{\text{c.m.}} = 13.4^\circ$) exit channels. The excitation energies of the residual states in ^{26}Mg are indicated. The solid line (see Sec. III) shows the location of nonstatistical structure.

tistical consideration that one such event would be likely out of n points. Others²⁸ have also chosen a probability of 0.01 as a cutoff but it is obvious that the smaller the probability $P(N)$ for an event, the more confident we are that the corresponding structure is nonstatistical.

The last test which we find useful is simply the sum of the excitation functions. It is expected that in a sum over many exit channels, the normal, Ericson-type fluctuations will average out while any correlated, nonstatistical structures will combine to form a peak. The sum suffers the same limitation as the deviation function in that a highly correlated structure will not be readily seen if the absolute magnitude of the enhancement in the individual excitation functions happens to be small. Another possibility is that if one excitation function has a large cross section relative to the other

excitation functions, it may dominate the sum and thereby obscure detailed structure contributed by all of the excitation functions.

We have found the distribution of maxima test to be the most useful overall, primarily because it allows a direct comparison to the statistical model. The sum, $C(E)$ and $D(E)$ functions are helpful for determining the centroid and width of a structure, although they are somewhat redundant.

The distribution of maxima test as well as the $C(E)$ and $D(E)$ functions make use of the running average $\langle \sigma_i(E) \rangle$. We have found that an averaging interval of $E_{\text{int}} \approx 3$ MeV (c.m.) is sufficient to remove the effects of the gross energy dependence from each excitation function. This removal of energy dependence is equivalent to requiring that the background part of the scattering matrix be constant with energy; this being a basic assumption of

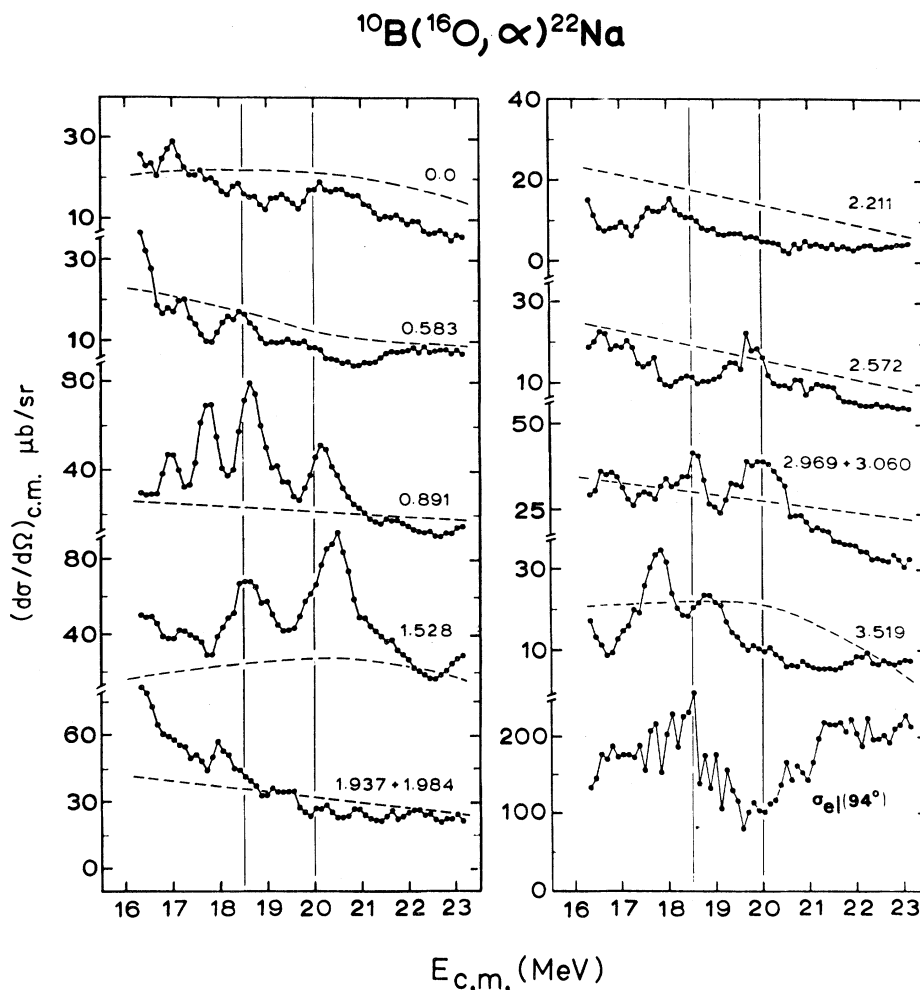


FIG. 5. Excitation functions for the $^{16}\text{O} + ^{10}\text{B}$ reaction for the elastic ($\theta_{\text{c.m.}} = 94^\circ$) and α -particle ($\theta_{\text{c.m.}} = 14.6^\circ$) exit channels. The excitation energies of the residual states in ^{22}Na are indicated. States with isospin $T = 1$ (0.657 and 1.952 MeV) are not populated. The solid lines (see Sec. III) show the location of nonstatistical structure. The dashed curves are Hauser-Feshbach calculations as described in the text.

the statistical model. Another criterion of the statistical model is that $\Gamma_J/D_J \gg 1$, where Γ_J is the mean width of compound nuclear states and D_J is the level spacing for spin J . Normally, at the high excitation energies considered here, it is assumed that this criterion is fulfilled. However, we have intentionally chosen entrance channels which bring in a great deal of angular momentum so that the actual number of available states may be quite small for the high spins (see the discussion in Sec. IV). Thus Γ_J/D_J may really be on the order of unity or even less, thereby disallowing the comparison of these data with statistical model expectations. In any case, the tests we have discussed here are enlightening because of their capacity to dis-

cern correlated structures in the data.

Another concern in applying the tests which use the running average is how to calculate $\langle \sigma_i(E) \rangle$ at energies within $E_{\text{int}}/2$ of the two end points of the excitation functions. Normally, $\langle \sigma_i(E) \rangle$ at a given point is found by averaging all data points within $\pm E_{\text{int}}/2$ of that point. However, for data points at energy $E_{\text{min}} < E < E_{\text{min}} + E_{\text{int}}/2$ or $E_{\text{max}} - E_{\text{int}}/2 < E < E_{\text{max}}$, the average cannot be calculated over the entire interval of length E_{int} . As a result, some problems may arise if the average cross sections of several excitation functions are not very constant with energy. For example, if the cross section is going steadily down with energy at the upper end point, E_{max} , then the running

average calculated at E_{\max} will be overestimated. This may occasionally cause spurious results, but these can be recognized as such by careful scrutiny of the excitation functions.

The numerical results of the relevant tests are summarized in Table II. Events with probabilities less than 0.01 are listed along with the experimental width Γ_{exp} (FWHM), the expected width of statistical fluctuations²⁹ Γ_{st} , and $\tau = \hbar/\Gamma_{\text{exp}}$. The sum, $C(E)$ and $D(E)$ seen in Figs. 6–8 are derived from the excitation functions corresponding only to the α -particle exit channels (except those which are incomplete), because the elastic excitation functions are generally lacking in structure.

B. Results for $^{17}\text{O} + ^{12}\text{C}$

The results for the $^{12}\text{C}(^{17}\text{O},\alpha)^{25}\text{Mg}$ reaction are seen in Fig. 6(a), where the sum is seen to exhibit considerable fluctuations. One might expect a smoother $1/E$ dependence after summing over 13 states with a reduction in the number of extrema compared to the individual excitation functions. However, calculations based on the treatment of van der Woude³⁰ show that this reduction has a surprisingly weak dependence upon the number of effective channels. We find the number of maxima in the sum in Fig. 6(a) to be consistent with the results of van der Woude, but the amplitudes are still surprising. In summed excitation functions, the statistical fluctuations are expected to be damped by a factor approximately equal to the number of levels summed.^{31,32} An examination of Fig. 6(a) shows that the fluctuations exceed this prediction.

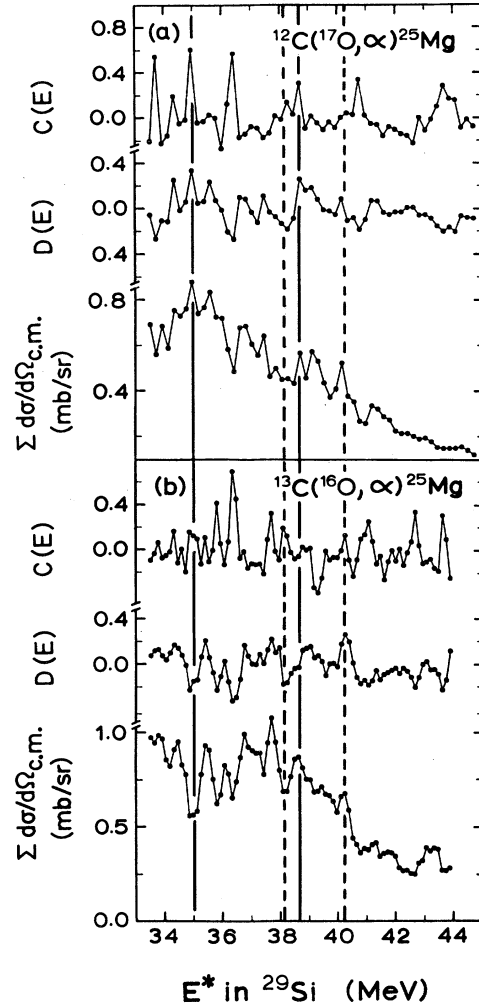


FIG. 6. Results of the sum, $C(E)$ and $D(E)$ tests for (a) the $^{12}\text{C}(^{17}\text{O},\alpha)^{25}\text{Mg}$ reaction and (b) the $^{13}\text{C}(^{16}\text{O},\alpha)^{25}\text{Mg}$ reaction. The solid (dashed) lines indicate the location of nonstatistical structure in the $^{17}\text{O} + ^{12}\text{C}$ ($^{16}\text{O} + ^{13}\text{C}$) system.

TABLE II. Candidates for nonstatistical structure in the four reactions studied.

Reaction	$E_{\text{c.m.}}$ (MeV)	E^* (MeV)	Probability	Γ_{exp} (keV)	$\Gamma_{\text{st}}^{\text{a}}$ (keV)	τ (10^{-21} sec)	$t_{\text{coll}}^{\text{b}}$ (10^{-22} sec)
$^{17}\text{O} + ^{12}\text{C}$	13.9	34.9	2×10^{-3}	~ 400	195	1.6	5.9
	17.6	38.7	3×10^{-3}	~ 400	240	1.6	5.6
$^{16}\text{O} + ^{13}\text{C}$	17.8	38.1	1×10^{-3}	~ 250	230	2.6	5.4
	19.9	40.2	6×10^{-3}	~ 300	260	2.2	5.3
$^{17}\text{O} + ^{13}\text{C}$	17.3	44.1	7×10^{-4}	~ 500	240	1.3	5.3
$^{16}\text{O} + ^{10}\text{B}$	18.5	38.0	5×10^{-3}	~ 400	290	1.6	5.2
	20.0	39.5	7×10^{-3}	~ 500	310	1.3	5.1

^aExpected width for statistical structure from Ref. 29.

^bApproximate collision time.

The two solid lines in Fig. 6(a) indicate energies at which correlated nonstatistical structures appear. The one at $E^* (^{29}\text{Si})=34.9$ MeV has a distribution of maxima probability of 2×10^{-3} and the one at $E^* (^{29}\text{Si})=38.7$ MeV has a distribution of maxima probability of 3×10^{-3} . The location of these structures is also indicated by the solid lines in Fig. 2 at $E_{\text{c.m.}}=13.9$ and 17.6 MeV. The low probability of the structure at $E_{\text{c.m.}}=13.9$ MeV comes about because six of the seven possible α groups have a peak near that energy. Some enhancement is seen in the elastics also, but it is rather weak and inconclusive. The structure at $E_{\text{c.m.}}=17.6$ MeV is not as pronounced because there are only about five peaks near the energy and some of them are weak and shifted slightly. Again the elastics do not show a significant correlation.

The $C(E)$ result in Fig. 6(a) shows additional correlations near 33.8, 36.5, and 43.5 MeV corresponding to $E_{\text{c.m.}}=12.7$, 15.4, and 22.4 MeV. However, the distribution of maxima probability calculations at these energies are not lower than 10^{-2} . At 12.7 MeV in Fig. 2 there is nothing apparent which would cause a large correlation; it is likely due to the end point problem with $\langle \sigma_i(E) \rangle$. At 15.4 MeV in Fig. 2, there are a few fairly strong peaks which may have caused the enhancement in $C(E)$. However, since the distribution of maxima probability depends only on the number of maxima, this event is not in disagreement with the statistical model. Some enhancement is visible near 22.4 MeV in Fig. 2 but, again, $C(E)$ may be influenced by the end point problem.

The widths of the two structures in the $^{17}\text{O} + ^{12}\text{C}$ system are difficult to assess. Although the sum shows the peaks to be only about one point wide, even a cursory inspection of the individual excitation functions shows that the peaks are closer to two points wide or 400 keV (all widths will be quoted as FWHM and in c.m. energy). It is also important to note there that we have repeated the runs near $E_{\text{c.m.}}=13.9$ and 17.6 MeV. The enhancement in the excitation functions and in their sum was well reproduced, thus giving us more confidence that these structures are not simply experimental aberrations. In summary, we may state that the respective probabilities are small enough to be in a disagreement with the statistical model according to our criteria. Although the two structures do not strongly dominate the excitation functions, they are reproducible and correlated, and therefore probably represent some type of real physical process such as a resonance.

C. Results for $^{16}\text{O} + ^{13}\text{C}$

Figure 6(b) shows the statistical test results for the $^{13}\text{C}(^{16}\text{O},\alpha)^{25}\text{Mg}$ reaction. Again, the rather sharp, Ericson fluctuations appear in the sum over the same 13 states of ^{25}Mg which were considered in the $^{12}\text{C}(^{17}\text{O},\alpha)^{25}\text{Mg}$ reaction. The dashed lines in Fig. 6(b) show the location of two possible nonstatistical structures, a minimum ($P=1 \times 10^{-3}$) at $E^* (^{29}\text{Si})=38.1$ MeV and a maximum ($P=6 \times 10^{-3}$) at $E^* (^{29}\text{Si})=40.2$ MeV. In Fig. 3 these structures are also indicated by the solid lines at $E_{\text{c.m.}}=17.8$ MeV, where six of the eight excitation functions have a minimum, and $E_{\text{c.m.}}=19.9$ MeV, where seven of the eight excitation functions have a maximum. The elastic excitation functions for the $^{16}\text{O} + ^{13}\text{C}$ reaction have some noticeable structure but none that is favorably correlated with the extrema seen in the α -particle exit channel.

The two structures in the $^{13}\text{C}(^{16}\text{O},\alpha)^{25}\text{Mg}$ reaction have similar widths, $\Gamma_{\text{exp}}=200-300$ keV. As in the preceding case, the probabilities do not disagree strongly with the statistical model, but they are outside our prescription for "normal" behavior.

D. Results for $^{17}\text{O} + ^{13}\text{C}$

Statistical test results for the $^{13}\text{C}(^{17}\text{O},\alpha)^{26}\text{Mg}$ reaction are shown in Fig. 7(a). The fluctuations in the sum in this case span several data points instead of only one or two. Only the maximum at $E^* (^{30}\text{Si})=44.1$ MeV [solid line in Fig. 7(a)] showed evidence for being nonstatistical. In examining Fig. 4, the enhancement at $E_{\text{c.m.}}=17.3$ MeV is clearly seen in seven of the eight groups in the α -particle exit channel. Because of this strong correlation, the calculated probability is 7×10^{-4} . The elastic scattering is quite smooth overall, with no correlation near $E_{\text{c.m.}}=17.3$ MeV.

The structure at $E^* (^{30}\text{Si})=44.1$ MeV in the $^{17}\text{O} + ^{13}\text{C}$ system is fairly broad, having $\Gamma_{\text{exp}} \simeq 500$ keV. The probability of this event is well outside of the 0.01 cutoff and the exit channel correlations are clearly visible. This structure represents the strongest candidate for a resonance in all of the present data.

E. Results for $^{16}\text{O} + ^{10}\text{B}$

The results for the last reaction, $^{10}\text{B}(^{16}\text{O},\alpha)^{22}\text{Na}$, are shown in Fig. 8(a). The solid lines indicate the

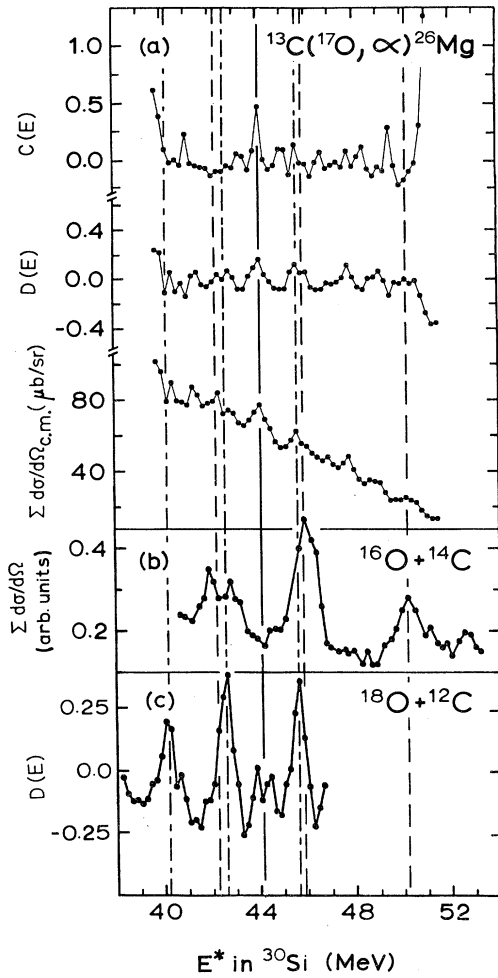


FIG. 7. (a) Results of the sum, $C(E)$ and $D(E)$ tests for the $^{13}\text{C}(^{17}\text{O}, \alpha)^{26}\text{Mg}$ reaction. The solid line indicates the location of a nonstatistical maximum. (b) Results from the sum of elastic scattering at eight angles for the $^{16}\text{O} + ^{14}\text{C}$ reaction, where the dashed lines indicate the resonances reported in Ref. 17. (c) Deviation function for elastic scattering at eight angles for the $^{18}\text{O} + ^{12}\text{C}$ reaction, where the dotted-dashed lines indicate the resonances reported in Ref. 18.

location of two possible nonstatistical maxima at $E^* (^{26}\text{Al}) = 38.0$ and 39.5 MeV. It is possible that there is a minimum near $E^* (^{26}\text{Al}) = 42.1$ MeV, as the correlation in $C(E)$ shows. In fact, the distribution of maxima probability is 2×10^{-3} . However, careful examination of the individual excitation functions in Fig. 5 shows that the correlations and probability calculations at $E_{c.m.} = 22.5$ MeV are not absolutely reliable because $\langle \sigma_i(E) \rangle$ used in these calculations is probably overestimated at that point. It can be seen from Fig. 5 that only three

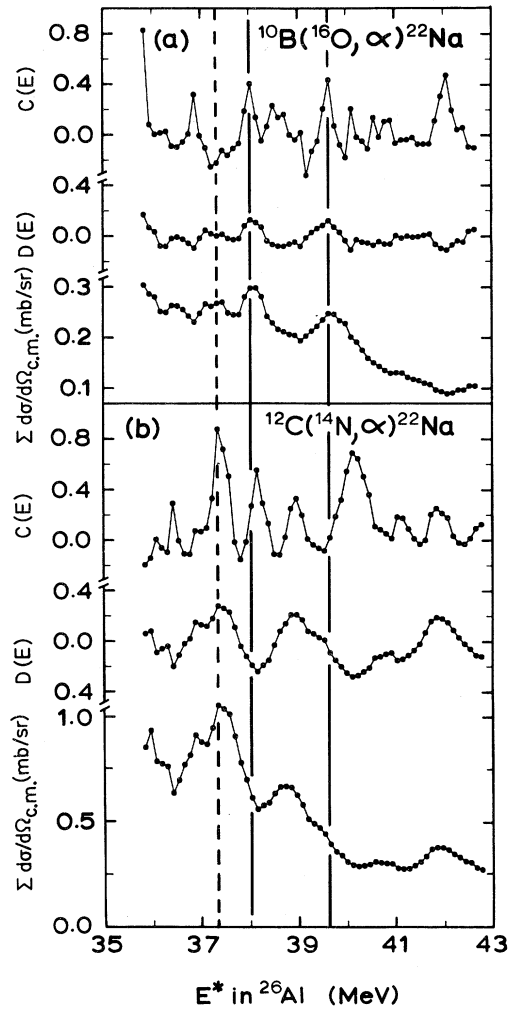


FIG. 8. Results of the sum, $C(E)$ and $D(E)$ tests for (a) the $^{10}\text{B}(^{16}\text{O}, \alpha)^{22}\text{Na}$ reaction and (b) the $^{12}\text{C}(^{14}\text{N}, \alpha)^{22}\text{Na}$ reaction (Ref. 12). The solid (dashed) lines indicate the location of nonstatistical structure in the $^{16}\text{O} + ^{10}\text{B}$ ($^{14}\text{N} + ^{12}\text{C}$) system.

or four of the nine groups have a minimum near $E_{c.m.} = 22.5$ MeV. We cannot rule out the possibility that this is a real minimum, but we cannot make a strong statement either way since it is too near to the end point. On the other hand, the two maxima are visible in the majority of the excitation functions, as shown by the solid lines at $E_{c.m.} = 18.5$ and 20.0 MeV in Fig. 5. At each of these two energies there are six or seven peaks out of a possible nine. The probabilities are 5×10^{-3} (18.5 MeV) and 7×10^{-3} (20.0 MeV). These probabilities are not very low, but this may be due to slight shifts of the peak locations in the excitation func-

tions.

The elastic scattering actually correlates with the maximum at $E_{c.m.} = 18.5$ MeV, but this may be a coincidence. The statistics for the elastic scattering in this case are somewhat poor ($\sim 15\%$), as evidenced by the severe fluctuations.

The two structures at $E_{c.m.} = 18.5$ and 20.0 MeV meet our criteria for being nonstatistical, but they are not as strong as the highly correlated structure in the $^{17}\text{O} + ^{13}\text{C}$ system. Their widths are somewhat uncertain because the peaks in the individual excitation functions are broader than what is seen in the sum. The structure at $E^* (^{26}\text{Al}) = 38.0$ MeV has a width $\Gamma_{\text{exp}} \simeq 350 - 450$ keV, while the one at $E^* (^{26}\text{Al}) = 39.5$ MeV is broader with $\Gamma_{\text{exp}} \simeq 400 - 600$ keV.

Overall we see that all four reactions show some evidence (of varying strength) for nonstatistical behavior in the α -particle exit channel. It is difficult to make definitive statements as to whether the structures seen are resonances because of the intrinsic nature of the measurements and tests. If we ask a statistical question, then we must expect to receive a statistical answer. For example, if we ask what the probability is that the structure at $E^* (^{29}\text{Si}) = 38.1$ MeV will occur in the set of $^{13}\text{C}(^{16}\text{O}, \alpha)^{25}\text{Mg}$ excitation functions, the answer is $P \sim 1 \times 10^{-3}$. This literally means that one time out of 1000, such a structure can and may occur. Therefore, we do not claim absolutely that the structures identified in Table II are resonances; we indicate simply that they are good candidates based on our statistical tests.

We have calculated the expected width for statistical fluctuations using the empirical formula of Stokstad,²⁹ $\Gamma_{\text{st}} = 14 \exp[-4.69(A/E^*)^{1/2}]$ MeV, where A is the mass number of the compound nucleus and E^* is the excitation energy in MeV. These results are presented in Table II, where it is seen that $\Gamma_{\text{exp}} \geq \Gamma_{\text{st}}$ in each case. In the $^{16}\text{O} + ^{13}\text{C}$ reaction $\Gamma_{\text{exp}} \simeq \Gamma_{\text{st}}$, but since the structures are fairly weak, no obvious conclusion is apparent. For the most part, the experimental widths for the suspected structures are larger than what would be expected for statistical fluctuations, thus providing further evidence that the structures seen are nonstatistical.

Table II also shows the approximate collision time t_{coll} for each reaction corresponding to the energies where structures were seen. Comparing the lifetime τ of the states listed to t_{coll} , we see that $\tau \simeq 3 - 4 \times t_{\text{coll}}$. This indicates that we may be seeing some type of short-lived intermediate structure,

since the lifetimes are longer than those for direct reactions ($\sim 10^{-21}$ sec) and shorter than those for a classical, long-lived, equilibrated compound nucleus ($\sim 10^{-16} - 10^{-20}$ sec).

IV. DISCUSSION

A. Comparison of models with experimental results

A variety of models have been proposed which deal with resonance phenomena and the more recent suggestions increasingly support the importance of the entrance channel properties. This is in contrast with some earlier concepts which tended to emphasize the properties of the compound nucleus above all else.

For example, Pocanic and Cindro³³ developed a model which depended only on the density of compound nuclear states. They used the conventional Fermi-gas model to calculate level densities, which does not allow one to differentiate between nuclides with the same A . In fact, no properties of the entrance channel were considered. This model predicted, for example, that ^{26}Al would be a poor candidate for resonances regardless of the entrance channel employed. This is now in contradiction with the strong resonances seen at $E^* (^{26}\text{Al}) = 25.5$ and 37.5 MeV populated via the $^{14}\text{N} + ^{12}\text{C}$ entrance channel.^{7,12}

Subsequently, Cindro and Pocanic³⁴ modified their model to include the consideration of properties of the entrance channel nuclei, especially the binding energy. They now suggest that resonances are most observable in systems where the rotational band defined by

$$E^* = E_0 + \frac{\hbar^2}{2I_{\text{eff}}} J(J+1) \quad (4)$$

falls within the molecular-resonance window defined by a zone of low level density. In practice, this criterion is met for composite systems with low level density and when the two incoming nuclei have low binding energies, as has been shown by Thornton *et al.*¹⁹

Recently Baye²⁰ formulated a simple rule for observing resonances associated with a weakening absorption for certain partial waves. For a given partial wave, this absorption is only important for channels with an effective (Coulomb plus centrifugal) barrier which is lower than the effective elastic barrier. The resulting implication is that, among

other things, some properties related to the entrance channel, such as the Q value and reduced mass, are important. However, since Baye applied the barrier rule to compound systems with $36 < A < 76$, we have no prediction for the nuclei considered in this paper.

The model proposed by Thornton *et al.*¹⁹ suggests that the binding energies of the entrance channel nuclei and, to a lesser extent, their moment of inertia at grazing distance, are the most important factors in determining which systems will resonate. If the binding energies of the incoming nuclei are high, then the separation energy S of the entrance channel from the compound nucleus will be low. As a result, the $E_{c.m.}$ needed to excite the compound nucleus to a given $E^* = E_{c.m.} + S$ will be larger than it would be if the binding energies were low. A larger $E_{c.m.}$ means more angular momentum is brought into the reaction, thereby increasing the probability of populating a semi-isolated, high-spin state. Such a state might be semi-isolated because, although the absolute density of states may be high, the number of states able to conserve total angular momentum and parity may be quite small for spin values near the grazing wave. The essence of this concept is that the level density at a given E^* in the compound nucleus depends critically on the binding energies of the incoming nuclei because l_{gr} depends indirectly on the separation energy.

It is possible to use this model to select which entrance channels are most likely to populate resonances in a compound nucleus. At a given E^* , the channel with the largest J will be the best candidate because the level density will be the lowest. This is clearly seen in Fig. 9, where the yrast and l_{gr} lines are shown for the three compound nuclei under investigation in this work. The yrast lines are derived using the spectral moment method of Ayik and Ginocchio³⁵ (see Ref. 19 for more details), except in the case of ^{30}Si , for which reliable level densities were unavailable. The l_{gr} lines are the various entrance channels are calculated using the Wilczynski formalism,²⁴ which we feel is adequate for energies above the Coulomb barrier.

In Fig. 9(c) it is evident that for a given E^* (^{26}Al), the $^{14}\text{N} + ^{12}\text{C}$ entrance channel brings in the most angular momentum. On the other hand, the $^{16}\text{O} + ^{10}\text{B}$ channel brings in considerably less, making it less likely to populate semi-isolated states in ^{26}Al . However, the channel spins play a role here. Because the orbital angular momentum and intrinsic spin add vectorially for form the total angular

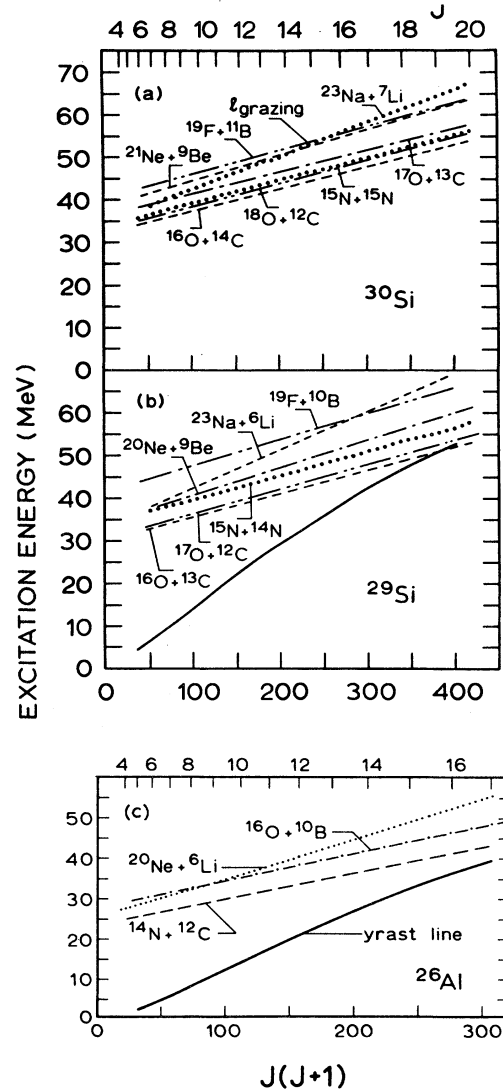


FIG. 9. Excitation energy in the compound nucleus versus $J(J+1)$ for spin states J in (a) ^{30}Si , (b) ^{29}Si , and (c) ^{26}Al . The solid lines are calculated yrast lines while the patterned lines show the grazing angular momentum for various entrance channels [plotted versus $l(l+1)$].

momentum, the $^{16}\text{O} + ^{10}\text{B}$ reaction will populate a distribution of states with up to $2s+1=7$ J values ($J_{\max} \simeq l_{gr} + 3$), while for the $^{14}\text{N} + ^{12}\text{C}$ channel the flux is only spread over $2s+1=3$ J values ($J_{\max} \simeq l_{gr} + 1$). This means that the resonance term in the cross section is damped by a factor of $1/(2s+1)$ or, in this case, $\frac{1}{7}$ versus $\frac{1}{3}$. Therefore, the $^{14}\text{N} + ^{12}\text{C}$ channel not only populates higher spin states than the $^{16}\text{O} + ^{10}\text{B}$ channel at a given E^* , but also fewer different spin states. The prediction then is that resonances are more likely to

be seen in the $^{14}\text{N} + ^{12}\text{C}$ reaction and they should be stronger than what would be expected in the $^{16}\text{O} + ^{10}\text{B}$ reaction.

Our experimental results are in good agreement with the arguments presented above. For the $^{10}\text{B}(^{16}\text{O},\alpha)^{22}\text{Na}$ reaction we find only weak evidence for resonances in the form of two semicorrelated structures with probabilities of 5×10^{-3} and 7×10^{-3} . However, results for the $^{12}\text{C}(^{14}\text{N},\alpha)^{22}\text{Na}$ reaction¹² show at least one strong resonance at $E^*(^{26}\text{Al}) = 37.5$ MeV ($P = 2 \times 10^{-4}$). Therefore, at least in the excitation energy range studies [$E^*(^{26}\text{Al}) = 35.8 - 42.6$ MeV], the experimental evidence and our model predictions are consistent.

Looking at Fig. 9(b) it can be seen that the $^{17}\text{O} + ^{12}\text{C}$ and $^{16}\text{O} + ^{13}\text{C}$ entrance channels are closely matched, at least in terms of l_{gr} . In fact, at $E^*(^{29}\text{Si}) = 40$ MeV, even the $J_{\text{max}} \simeq l_{\text{gr}} + s$ are similar ($\sim 15\hbar$ for $^{17}\text{O} + ^{12}\text{C}$ and $\sim 14\hbar$ for $^{16}\text{O} + ^{13}\text{C}$). Thus we would expect the probability for populating resonances via these entrance channels to be comparable. We would also expect the strength of any structures seen in the $^{17}\text{O} + ^{12}\text{C}$ channel to be damped compared to those in the $^{16}\text{O} + ^{13}\text{C}$ channel ($\frac{1}{6}$ versus $\frac{1}{2}$), since the channel spins are $\frac{5}{2}$ and $\frac{1}{2}$, respectively.

The experimental results for the ^{29}Si compound nucleus (Table II) are indeed quite similar for the two entrance channels. There are two structures in each channel with probabilities near 2×10^{-3} , although the widths of the structures in the $^{17}\text{O} + ^{12}\text{C}$ system are somewhat larger than those in the $^{16}\text{O} + ^{13}\text{C}$ system.

The last case at hand is the ^{30}Si compound nucleus. Figure 9(a) shows that the $^{16}\text{O} + ^{14}\text{C}$, $^{18}\text{O} + ^{12}\text{C}$, $^{15}\text{N} + ^{15}\text{N}$, and $^{17}\text{O} + ^{13}\text{C}$ entrance channels are all good candidates for populating high-spin states. The $^{16}\text{O} + ^{14}\text{C}$ and $^{18}\text{O} + ^{12}\text{C}$ reactions have been previously studied (Refs. 17 and 18), with several resonances having been seen in both, particularly in the elastic scattering. Also of importance is the fact that the resonances reported in those systems are among the largest ever observed in systems not comprised exclusively of α -like nuclei. Both results, the observance and strength of the resonances in the $^{16}\text{O} + ^{14}\text{C}$ and $^{18}\text{O} + ^{12}\text{C}$ systems, are consistent with our model, since Fig. 9(a) shows that these two channels are the best candidates for populating resonances. The strength of the resonances follows from the fact that both channels have no intrinsic spin and thus no damping of the resonance part of the cross section.

We have studied the $^{13}\text{C}(^{17}\text{O},\alpha)^{26}\text{Mg}$ reaction over an excitation energy range common to both the $^{16}\text{O} + ^{14}\text{C}$ and $^{18}\text{O} + ^{12}\text{C}$ data. Our model would predict the $^{17}\text{O} + ^{13}\text{C}$ entrance channel to be a reasonably good candidate for populating resonances, but not as good as the other two channels mentioned. Also the strength of an observed resonance should be relatively damped by a factor of $\frac{1}{7}$ (maximum channel spin is $3\hbar$). Our measurements show one structure of reasonable strength ($P = 7 \times 10^{-4}$) in the energy region studied. Certainly this must be considered as consistent with the present model.

B. Reaction mechanisms

One of the goals of this work was to see if the population of resonances could be effected through closely matched entrance channels which bring in comparable amounts of total angular momentum when forming a compound nucleus at the same E^* . Although it is effectively impossible to find entrance channels which are matched exactly, the ones we chose to examine are indeed well matched.

The details of the close l matching of the $^{17}\text{O} + ^{12}\text{C}$ and $^{16}\text{O} + ^{13}\text{C}$ channels leading to ^{29}Si have been discussed in Sec. IV A. However, we see from Fig. 6 that the lines indicating where nonstatistical structures were identified in the two entrance channels do not coincide. We can also see from Figs. 2 and 3 that the structure in the individual excitation functions is not the same for the two channels. Therefore, the same nuclear states are apparently not populated through these two entrance channels.

Figure 7 compares three different entrance channels for the ^{30}Si compound nucleus. The solid line locates the structure we see in the $^{17}\text{O} + ^{13}\text{C}$ system at $E^*(^{30}\text{Si}) = 44.1$ MeV, the dashed lines show the structures reported in the $^{16}\text{O} + ^{14}\text{C}$ system by Bernhardt *et al.*,¹⁷ and the dashed-dotted lines show the structures seen by Webb *et al.*¹⁸ in the $^{18}\text{O} + ^{12}\text{C}$ system. At $E^*(^{30}\text{Si}) = 42.4$ and 45.0 MeV there are peaks in the $^{16}\text{O} + ^{14}\text{C}$ and $^{18}\text{O} + ^{12}\text{C}$ systems which almost align. So although there seems to be some correlation between two of the channels, there is clearly no energy at which all three channels exhibit a structure.

We find a similar result in the ^{26}Al system, where the structures seen in the $^{16}\text{O} + ^{10}\text{B}$ ($^{14}\text{N} + ^{12}\text{C}$) channel are indicated by the solid (dashed) lines. It is obvious that none of the structures in the two channels occur at the same energy.

Again, the l matching here is quite good. Although Fig. 9(c) shows that the $^{14}\text{N} + ^{12}\text{C}$ channel brings in the more angular momentum than the $^{16}\text{O} + ^{10}\text{B}$ channel, J_{max} is similar in both cases since the channel spins are $1\hbar$ and $3\hbar$, respectively. In addition, comparing the structure of the $^{16}\text{O} + ^{10}\text{B}$ excitation functions to that of the $^{14}\text{N} + ^{12}\text{C}$ reaction in Ref. 12, we see a great dissimilarity.

To summarize, we see little or no evidence that we are populating the same nonstatistical structures through different entrance channels to the same compound nucleus. In addition, in the two systems for which we have excitation functions for the same particles and energies (^{26}Al and ^{29}Si), we may state more generally that we are not populating precisely the same nuclear states either, because the individual excitation functions are dissimilar.

This result is somewhat surprising in light of the following argument. Admittedly, although we are making comparisons at the same excitation energy, the angular momenta brought in by each entrance channel are close but not exactly the same. However, since we have nonzero channel spin in most cases, these reactions actually bring in a different distribution of total J , due in part to the possible spin projections of \vec{s} onto \vec{l} . The result is a large overlap of the total J brought into the reaction. For example, at E^* (^{26}Al) = 40 MeV, we calculate $l_{\text{gr}} = 15.3\hbar$ ($12.9\hbar$) for the $^{14}\text{N} + ^{12}\text{C}$ ($^{16}\text{O} + ^{10}\text{B}$) channel, with the respective channel spins being $1\hbar$ and $3\hbar$. Thus for the grazing wave, we have $14.3\hbar < J < 16.3\hbar$ for $^{14}\text{N} + ^{12}\text{C}$ and $9.9\hbar < J < 15.9\hbar$ for $^{16}\text{O} + ^{10}\text{B}$. One would expect that, with $J_{\text{max}} \simeq 16\hbar$ for each channel, very nearly the same nuclear states would be populated in ^{26}Al by each channel. This argument also holds for the other two compound nuclei. Furthermore, if the nonstatistical structures we see are really due to semi-isolated states of high spin which are populated only when \vec{l} and \vec{s} are aligned (i.e., by $J_{\text{max}} \simeq l_{\text{gr}} + s$), then we really do expect to see these states in each entrance channel with comparable intensity except for the $1/(2s + 1)$ damping. Also, since the energy-dependent cross-correlation function searches for *correlations* without a strong dependence on relative intensity, we are indeed capable of detecting such states in the excitation functions.

A number of implications arise from the fact that we are not populating the same nuclear states through similar entrance channels. One possibility is that the nonstatistical structures we see are semi-isolated, high-spin, compound nuclear states

which can only be excited by a particular combination of E^* and J^π . The elastic scattering provides further evidence that the reaction mechanism might be compound nuclear. Hauser-Feshbach calculations show that most of the elastic scattering at $\theta_{\text{lab}} = 34^\circ$ is shape elastic, not compound. Thus, we would not expect to see effects of a resonance in the compound nucleus in the elastic scattering. Indeed, we find no correlation in the elastic channel with the structures seen in the α -particle exit channel (see Sec. III).

Another possible reaction mechanism which is consistent with our results is that of a quasimolecule. It has been shown that some observed resonances represent quasistable states formed by the colliding ions. These states may subsequently decay into a compound nucleus, elastic channel, inelastic channel, or some other exit channel. It is clear that since they form different molecules with different J , we would not expect the various entrance channels to resonate at the same equivalent excitation energy.

The existence of such states seems likely in the reactions considered here because of the high total angular momenta involved. The number of available states in the compound nucleus is very small for large J , so the system is almost forced into a quasimolecular configuration which is capable of absorbing the angular momentum. The decay of such a system is similarly governed by the large J in that it may only decay into channels which can carry away large angular momenta. Clearly the inelastic, elastic, and α -particle exit channels are good candidates for decay.

We have noted that no structures are seen in our elastic scattering measurements. However, this does not preclude the possibility that a quasimolecule is formed. It just implies that the dominant elastic process is shape elastic scattering. It seems reasonable that the cross section for the formation of a quasimolecule which decays back into the elastic channel must be considerably less than the cross section for shape elastic scattering. Therefore, we do not expect to see evidence for a quasimolecule in this channel.

On the other hand, if quasimolecular states are being formed, we would expect to see them in the α -particle exit channel. Since compound nucleus formation is not very favorable due to the large J , a large fraction of the events leading to the α channel would be due to formation and decay of a quasimolecule. Additional support for this idea is seen in Table II, where the widths of the states we

see are all greater than the predicted width for normal statistical (compound nuclear) fluctuations. Moreover, the lifetimes associated with these widths are roughly equal to the time for one rotation of the pertinent molecule. We also note that the theoretical predictions of Heenen and Baye³⁶ indicate that quasimolecular resonances can exist in non- α -conjugate systems. They did a multi-channel generator-coordinate study which predicted, for example, that $^{16}\text{O} + ^{14}\text{C}$ and $^{14}\text{C} + ^{14}\text{C}$ should resonate. Experiments on the $^{16}\text{O} + ^{14}\text{C}$ system¹⁷ are in agreement with this prediction.

Based on the evidence at hand, it is not altogether clear whether the nonstatistical structures we see are quasimolecular or compound nuclear. In fact, the question may not even be relevant for the high excitation energies and spins involved here. We know that, if one is formed at all, the compound nucleus must be highly deformed in order to exist with such large J values. Perhaps we are approaching a spin-energy regime in which an entrance channel quasimolecule and a highly deformed compound nucleus are one and the same.

V. CONCLUSIONS

We have conducted a search for nonstatistical structure in three non- α -conjugate systems (^{26}Al , $^{29,30}\text{Si}$) at high excitation energies ($30 < E^* < 50$ MeV). The experimental results for each system show evidence for nonstatistical, possibly resonant structures, correlated in many α -particle exit channels. No correlation is seen in the elastic exit channel. The existence of these structures greatly extends the number of non- α -conjugate systems in which possible resonances have been seen.

All of the experimental results discussed in Sec. IV support the idea that the actual density of states available (through a particular entrance channel and for spin J) in the compound system at a given E^* depends upon the properties of the entrance channel, especially the separation energy. By comparing the yrast line of a nucleus to the angular momentum brought into the reaction by various entrance channels, we have been able to select entrance channels which populate the highest spin states in the compound system. It has been shown that α -like reactants are most suitable for bringing in the most angular momentum at a given excitation energy due to their high binding (low separation) energies, thus explaining the great frequency with which resonances have been seen in α -like systems.

Although we suggest that the nonstatistical structures we see are due to semi-isolated, high-spin states populated by the largest available partial wave ($J_{\text{max}} \simeq l_{\text{gr}} + s$), we cannot be certain from our data that such states are compound nuclear or quasimolecular. We state only that we believe that they are states of the compound *system*. It is possible that the unavailability of very high-spin states *requires* that the colliding ions form a quasimolecule. If so, then this nuclear molecule could actually be viewed, in a certain sense, as a compound nuclear state. Certainly it would be a state of the compound system. The lifetimes of the states we see are consistent with the concept of a quasimolecule or a highly excited and, therefore, short-lived compound nucleus. We also point out that theoretical support for quasimolecules in non- α -conjugate nuclei has been reported by Heenen and Baye,³⁶ for example.

Although we have shown that we cannot populate the same nonstatistical structures (or nuclear states) through different entrance channels, this fact alone does not tell us absolutely whether these reactions proceed through a quasimolecule or a compound nucleus (or both). The only clear implication is that the nuclear states we populate are strongly dependent upon the entrance channel, even for channels which are closely matched in angular momentum.

It may be possible to ascertain the true reaction mechanism by studying more entrance and exit channels. Measuring angular distributions can be helpful because anomalies at backward angles have been associated with quasimolecular states as reported by Stokstad *et al.*³⁷ Measuring the spins of resonant structures is also quite informative, but this is nearly impossible in systems such as those considered here due to the nonzero channel spins involved.

In summary, it is suggested that the reaction mechanism responsible for the nonstatistical structures we see in several non- α -conjugate nuclei could be either quasimolecular or compound nuclear. Discriminating between these two processes may be immaterial, since a compound nuclear state with very high spin and excitation energy may be greatly deformed to the extent that it may be functionally equivalent to a nuclear molecule.

ACKNOWLEDGMENTS

The authors would like to thank collaborators R. Gyufko and G. Köhler for assistance during the

data acquisition phase of the experiment. Financial support from the U. S. National Science Foundation, the University of Virginia Computing Center, and the Max-Planck-Institut für Kernphy-

sik, Heidelberg are gratefully acknowledged. Two of the authors, K.R.C. and S.T.T., were supported in part by fellowships from NATO and the Fulbright-Hays Program, respectively.

- ¹D. A. Bromley, J. A. Kuehner, and E. Almqvist, *Phys. Rev. Lett.* **4**, 365 (1960).
- ²E. Almqvist, D. A. Bromley, and J. A. Kuehner, *Phys. Rev. Lett.* **4**, 515 (1960).
- ³D. A. Bromley, J. A. Kuehner, and E. Almqvist, *Phys. Rev.* **123**, 878 (1961).
- ⁴H. Voit, G. Ischenko, F. Siller, and H.-D. Helb, *Nucl. Phys.* **A179**, 23 (1972).
- ⁵D. J. Crozier and J. C. Legg, *Phys. Rev. Lett.* **33**, 782 (1974).
- ⁶R. A. Dayras, R. G. Stokstad, Z. E. Switkowski, and R. W. Wieland, *Nucl. Phys.* **A265**, 153 (1976).
- ⁷K. R. Cordell, S. T. Thornton, L. C. Dennis, P. G. Lookadoo, T. C. Schweizer, J. L. C. Ford, Jr., J. Gomez del Campo, and D. Shapira, *Nucl. Phys.* **A323**, 147 (1979).
- ⁸R. Middleton, J. D. Garrett, and H. T. Fortune, *Phys. Rev. C* **4**, 1987 (1971).
- ⁹D. Fick, in *Nuclear Molecular Phenomena*, edited by N. Cindro (North-Holland, Amsterdam, 1978), p. 269.
- ¹⁰P. Taras, in *Clustering Aspects of Nuclear Structure and Nuclear Reactions*, Proceedings of the Third International Conference on Clustering Aspects of Nuclear Structure and Nuclear Reactions, edited by W. T. H. Van Oers, J. P. Svenne, J. S. C. McKee, and W. R. Falk (A.I.P., New York, 1978), p. 234.
- ¹¹L. C. Dennis, S. T. Thornton, and K. R. Cordell, *Phys. Rev. C* **19**, 777 (1979).
- ¹²K. R. Cordell, C.-A. Wiedner, and S. T. Thornton, *Phys. Rev. C* **23**, 2035 (1981).
- ¹³L. C. Dennis, S. T. Thornton, K. R. Cordell, R. L. Parks, R. R. Doering, D. Shapira, J. Gomez del Campo, and J. L. C. Ford, Jr., *Nucl. Phys.* **A357**, 521 (1981).
- ¹⁴J. F. Mateja, A. D. Frawley, A. Roy, J. R. Hurd, and N. R. Fletcher, *Phys. Rev. C* **18**, 2622 (1978).
- ¹⁵A. D. Frawley, J. F. Mateja, A. Roy, and N. R. Fletcher, *Phys. Rev. Lett.* **41**, 846 (1978).
- ¹⁶J. Gomez del Campo, J. L. C. Ford, Jr., R. L. Robinson, M. E. Ortiz, A. Dacal, and E. Andrade, *Phys. Lett.* **69B**, 415 (1977).
- ¹⁷K. G. Bernhardt, H. Bohm, K. A. Eberhard, R. Vandenbosch, and M. P. Webb, in *Nuclear Molecular Phenomena*, edited by N. Cindro (North-Holland, Amsterdam, 1978), p. 367.
- ¹⁸M. P. Webb, R. Vandenbosch, K. A. Eberhard, K. G. Bernhardt, and M. S. Zisman, *Phys. Rev. Lett.* **36**, 779 (1976).
- ¹⁹S. T. Thornton, L. C. Dennis, and K. R. Cordell, *Phys. Lett.* **91B**, 196 (1980).
- ²⁰D. Baye, *Phys. Lett.* **97B**, 17 (1980).
- ²¹H. Hafner and H. H. Duhm, *Nucl. Instrum. Methods* **160**, 273 (1979).
- ²²J. Gomez del Campo, J. L. C. Ford, Jr., R. L. Robinson, P. H. Stelson, and S. T. Thornton, *Phys. Rev. C* **9**, 2148 (1974).
- ²³K. R. Cordell, S. T. Thornton, L. C. Dennis, T. C. Schweizer, J. Gomez del Campo, and J. L. C. Ford, Jr., *Nucl. Phys.* **A296**, 278 (1978).
- ²⁴J. Wilczynski, *Nucl. Phys.* **A216**, 386 (1973).
- ²⁵A. Gilbert and A. G. W. Cameron, *Can. J. Phys.* **43**, 1446 (1965).
- ²⁶C. M. Perey and F. G. Perey, *Nucl. Data* **A10**, 539 (1972).
- ²⁷L. R. Greenwood, K. Katori, R. E. Malmin, T. H. Braid, J. C. Stoltzfus, and R. H. Siemssen, *Phys. Rev. C* **6**, 2112 (1972).
- ²⁸R. A. Dayras, R. G. Stokstad, Z. E. Switkowski, and R. M. Wieland, *Nucl. Phys.* **A265**, 153 (1976).
- ²⁹R. G. Stokstad, *Proceedings of the International Conference on Reactions Between Complex Nuclei, Nashville, Tennessee* (North-Holland, Amsterdam, 1974), Vol. 2, p. 327.
- ³⁰A. van der Woude, *Nucl. Phys.* **80**, 14 (1966).
- ³¹J. P. Bondorf and R. B. Leachman, *Dan. Vidensk. Selsk., Mat-Fys. Medd.* **34**, No. 10 (1965).
- ³²W. R. Gibbs, *Phys. Rev.* **153**, 1206 (1967).
- ³³D. Pocanic and N. Cindro, *J. Phys. G* **5**, L25 (1979).
- ³⁴N. Cindro and D. Pocanic, *J. Phys. G* **6**, 359 (1980).
- ³⁵S. Ayik and J. N. Ginocchio, *Nucl. Phys.* **A234**, 13 (1974).
- ³⁶P.-H. Heenen and D. Baye, *Phys. Lett.* **81B**, 295 (1979).
- ³⁷R. Stokstad, D. Shapira, L. Chua, P. Parker, M. W. Sachs, R. Wieland, and D. A. Bromley, *Phys. Rev. Lett.* **28**, 1523 (1972).